Cell Reports

Report

BMP4 Gene Therapy in Mature Mice Reduces BAT Activation but Protects from Obesity by Browning Subcutaneous Adipose Tissue

Graphical Abstract

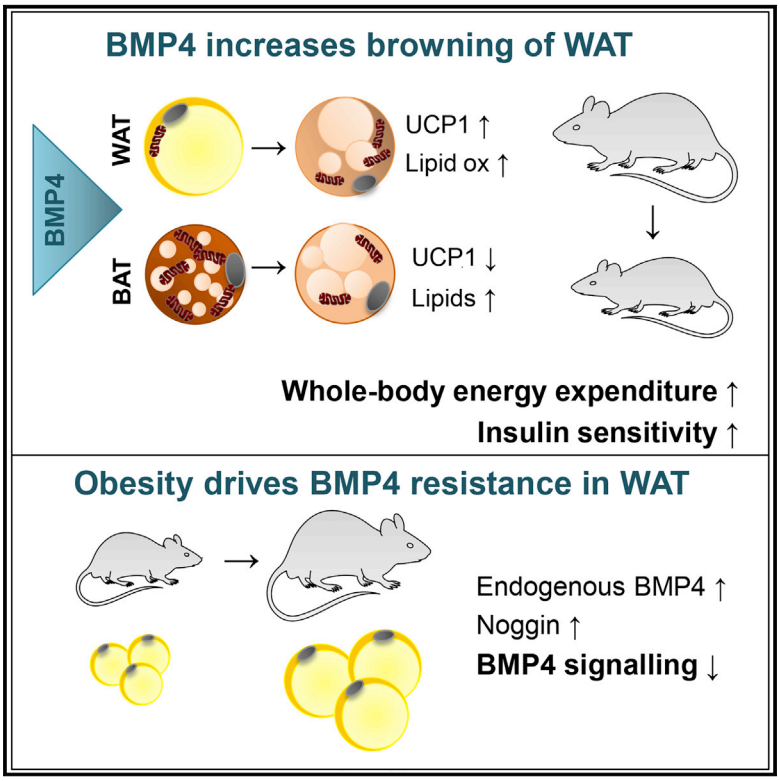

Highlights

- Increased circulating BMP4 in adult mice prevents obesity and insulin resistance
- Subcutaneous fat undergoes browning, and whole-body energy expenditure is increased
- BMP4 reduces BAT activation
- The results highlight the importance of browning subcutaneous fat

Authors

Jenny M. Hoffmann, John R. Grünberg, Christopher Church, ..., Ann Hammarstedt, Shahram Hedjazifar, Ulf Smith

Correspondence

ulf.smith@medic.gu.se

In Brief

Hoffmann et al. show that increased circulating BMP4 in mature mice targets subcutaneous WAT, promoting its browning with increased UCP1 and mitochondria and increased energy expenditure. Increased BMP4 also targets BAT, resulting in increased lipids and reduced UCP1. Together, these findings underscore the potential of browning WAT.

Hoffmann et al., 2017, Cell Reports *20*, 1038–1049
August 1, 2017
http://dx.doi.org/10.1016/j.celrep.2017.07.020

CellPress

OPEN ACCESS
CellPress

Cell Reports
Report

BMP4 Gene Therapy in Mature Mice Reduces BAT Activation but Protects from Obesity by Browning Subcutaneous Adipose Tissue

Jenny M. Hoffmann,[1] John R. Grünberg,[2] Christopher Church,[3] Ivet Elias,[4,5] Vilborg Palsdottir,[6] John-Olov Jansson,[6] Fatima Bosch,[4,5] Ann Hammarstedt,[1] Shahram Hedjazifar,[1] and Ulf Smith[1,7,*]

[1]The Lundberg Laboratory for Diabetes Research, Department of Molecular and Clinical Medicine, the Sahlgrenska Academy, University of Gothenburg, 405 30 Gothenburg, Sweden

[2]Metabolic Research Laboratories, Wellcome Trust MRC Institute of Metabolic Science, Addenbrooke's Hospital, University of Cambridge, Cambridge CB2 1TN, UK

[3]Cardiovascular and Metabolic Disease, MedImmune, Granta Park, Cambridge CB21 6GH, UK

[4]Center of Animal Biotechnology and Gene Therapy and Department of Biochemistry and Molecular Biology, School of Veterinary Medicine, Universitat Autònoma de Barcelona, 08193 Bellaterra, Barcelona, Spain

[5]Centro de Investigación Biomédica en Red de Diabetes y Enfermedades Metabólicas Asociadas (CIBERDEM), 08029 Madrid, Spain

[6]Department of Physiology/Endocrinology, the Sahlgrenska Academy, University of Gothenburg, 405 30 Gothenburg, Sweden

[7]Lead Contact

*Correspondence: ulf.smith@medic.gu.se

http://dx.doi.org/10.1016/j.celrep.2017.07.020

SUMMARY

We examined the effect of Bone Morphogenetic Protein 4 (BMP4) on energy expenditure in adult mature mice by targeting the liver with adeno-associated viral (AAV) BMP4 vectors to increase circulating levels. We verified the direct effect of BMP4 in inducing a brown oxidative phenotype in differentiating preadipocytes in vitro. AAV-BMP4-treated mice display marked browning of subcutaneous adipocytes, with increased mitochondria and Uncoupling Protein 1 (UCP1). These mice are protected from obesity on a high-fat diet and have increased whole-body energy expenditure, improved insulin sensitivity, reduced liver fat, and reduced adipose tissue inflammation. On a control diet, they show unchanged body weight but improved insulin sensitivity. In contrast, AAV-BMP4-treated mice showed beiging of BAT with reduced UCP1, increased lipids, and reduced hormone-sensitive lipase (HSL). Thus, BMP4 exerts different effects on WAT and BAT, but the overall effect is to enhance insulin sensitivity and whole-body energy expenditure by browning subcutaneous adipose tissue.

INTRODUCTION

Recent studies have demonstrated that there are two distinct variants of oxidative adipocytes. The classical brown adipocytes, present in the inter-scapular region of infants and other mammals, have a muscle-like Myogenic Factor (*MYF*) 5+, Paired Box Protein (*PAX*) 7+ cell-developmental origin (Seale et al., 2008). The second variant, beige adipocytes, is intermediate between brown and white adipocytes (Wang et al., 2013; Wu et al., 2012). These cells usually reside within white adipose tissue (WAT) depots (Vitali et al., 2012), have a white adipocyte stem-cell origin, and prevail in human brown adipose tissue (BAT) (Wu et al., 2012). Beige adipocytes have the capacity to generate heat by Uncoupling Protein 1 (UCP1)-dependent thermogenesis upon stimulation but also have other pathways for generating heat, including the recently described futile creatine cycle (Kazak et al., 2015), and secretion of a thermogenic SLIT2 fragment (Svensson et al., 2016). The potential of beige adipose cells in increasing energy expenditure in animals (Kazak et al., 2015; Seale et al., 2011; Wu et al., 2012) and in man (Sidossis et al., 2015) has been emphasized. Thus, activating the large subcutaneous (SubQ) WAT by browning seems an attractive way of preventing/treating obesity and type 2 diabetes.

A growing body of evidence has shown that Bone Morphogenetic Protein 4 (BMP4) is an important regulator of white adipogenesis by committing mesenchymal precursor cells into the adipogenic lineage and inducing Peroxisome Proliferator-Activated Receptor γ (PPARg) activation (Bowers and Lane, 2007; Gustafson and Smith, 2012). However, BMP4 also enhances browning of white adipocytes, as shown in transgenic mice overexpressing *Bmp4* in fat under the Adipocyte Protein 2 (*aP2*) promoter (Qian et al., 2013). Furthermore, we recently found that increasing BMP4 signaling through silencing the endogenous BMP4 inhibitor Gremlin1 induces browning of human SubQ (pre-)adipocytes with increased PPARγ Coactivator 1α (PGC1a), mitochondrial biogenesis, and other markers of browning (Gustafson et al., 2015).

Interestingly, the effect of increased BMP4 signaling seems different in primary brown adipose cells. These cells assume a less oxidative, white/beige-like phenotype, with larger lipid droplets associated with inhibition of lipolysis rather than the classical brown phenotype (Modica et al., 2016). Larger BAT with increased lipid droplet size was also reported in the *aP2*-driven *Bmp4* transgenic animal model (Qian et al., 2013), and, interestingly, human BAT has been reported to be mainly of a beige phenotype but

with some areas of maintained classical brown fat (Bartelt and Heeren, 2014; Jespersen et al., 2013; Wu et al., 2012). BMP4 has several important developmental effects that can confound results obtained in transgenic animal models. These developmental effects with early commitment and expansion of precursor cells with a primary beige/brown phenotype may well be important for the overall expansion of the beige/brown adipose tissue. If so, it raises the question of whether BMP4 is a possible target to treat or prevent obesity in adult human where developmental effects are unwanted. To address this, we examine here whether merely increasing circulating levels of BMP4 in adult mice, following gene therapy targeting the liver to increase BMP4 secretion, could be a potential therapeutic avenue.

RESULTS

Increased Circulating BMP4 Levels in AAV-BMP4-Treated Mice

The combination of AAV vectors of serotype 8 and the *hAAT1* promoter is well validated to ensure liver-specific transgene expression (Anguela et al., 2013; Zincarelli et al., 2008). Hepatic gene expression of the codon-optimized *Bmp4* sequence (data not shown) and hepatic BMP4 protein (Figure S1A) were increased, compared that in the controls. Serum BMP4 levels of the AAV BMP4 mice from Cohort 1 (Figure 1A) were increased around 10-fold (100–200 ng/mL) when examined in samples harvested 17 weeks post-AAV vector administration.

We also measured BMP4 protein in other tissues (SubQ WAT, BAT, and gastrocnemius skeletal muscle) but did not find the AAV vectors to target other tissues than the liver (Figure S1B), nor did increased circulating BMP4 enhance the endogenous expression of *Bmp2*, *Bmp7*, or *Bmp8B* (Figure S1C). These results demonstrate that the mice had increased circulating BMP4 levels with the AAV vectors and that the transgene expression lasted for the full duration of the study.

BMP4 Prevents Obesity in High-Fat-Diet-Fed Mice and Increases Energy Expenditure

Concurrent with AAV BMP4 vector administration in Cohort 1, the mice were allocated to either a control diet (CD) or a high-fat diet (HFD). The effect of BMP4 to reduce body-weight increase in the HFD-fed mice (HFD BMP4) was seen already after 2 weeks, and these mice gained less weight than the HFD controls during the entire study (Figure 1B). This was not caused by reduced food intake, and CD BMP4 mice had a significantly higher food intake than CD control mice did in Cohort 1 (Figure 1C). HFD BMP4 mice at week 17 did not have an increased food intake, compared to the HFD controls, but they also weighed considerably less (Figure 1C). These results demonstrate that AAV BMP4 mice were protected from diet-induced obesity, indicating that elevated BMP4 serum levels lead to changes in tissues regulating energy expenditure. For technical reasons, we could only examine energy expenditure in the mice in Cohort 2, which were treated similarly but only fed a CD after injecting the AAV BMP4 vectors at an even higher age than Cohort 1, i.e., at 12 weeks of age. Similar to Cohort 1, these mice weighed the same as the CD control mice (Figure 1D) and had significantly increased food intake (Figure 1E) and increased oxygen consumption and energy expenditure (both in Figure 1F). There was no difference in the activity of the mice (Figure S1D) or in core body temperature at room temperature (Figure S1E).

AAV BMP4 Mice Have Improved Glucose Tolerance and Insulin Sensitivity

To assess effects on glucose homeostasis, we performed an intraperitoneal insulin test and a glucose tolerance test (ITT and GTT, respectively). HFD BMP4 mice were more insulin sensitive than the control group (Figure 1G) and similar, in insulin sensitivity, to lean CD mice. Glucose tolerance was also significantly improved and similar to that in lean CD mice (Figure 1H), and circulating insulin levels at baseline and 15 min post-glucose injection were also lower (Figure 1I). Importantly, CD BMP4 mice with virtually identical body weights also demonstrated improved insulin sensitivity and glucose tolerance compared to the CD control group (Figures 1G and 1H). Thus, elevated BMP4 levels in fully mature mice produce a phenotype of increased energy expenditure, increased glucose tolerance, and insulin sensitivity in both CD- and HFD-fed mice, and elevated BMP4 levels protect from diet-induced obesity.

Elevated BMP4 Is Associated with Increased Lipid Accumulation in BAT

To explore mechanisms for BMP4, we first examined whether the skeletal muscles were targets but saw no increase in proteins of the mitochondrial oxidative phosphorylation (OXPHOS) pathway in either soleus or gastrocnemius muscles (Figures 2A and 2B). We then explored whether increased BMP4 in these adult, fully developed mice targeted WAT or BAT. In contrast to findings in *aP2*-driven *Bmp4* transgenic mice (Qian et al., 2013), BAT weight was not significantly altered in our mature HFD BMP4 mice (shown in Figure S2B), but UCP1 protein was significantly reduced (Figure 2C), while OXPHOS proteins (Figure 2D) were not apparently different in the BMP4 mice kept at room temperature. However, BAT in CD BMP4 mice with virtually identical body weights as the controls had increased expression of white adipocyte genes (Figure 2E) and increased lipids in BAT (Figure 2F), supporting the induction of a more beige phenotype with reduced lipid oxidation. Thus, BAT also is a target of BMP4 in these fully developed and mature mice. We then examined whether this increased accumulation of lipids was associated with markers of reduced upstream protein kinase A (PKA) activation, but phospho-PKA substrates were not changed (Figure 2G). However, the downstream lipolytic process is likely impaired, since hormone-sensitive lipase (HSL) protein in BAT was significantly reduced (Figure 2H), as also reported previously (Modica et al., 2016).

Taken together, increased circulating levels of BMP4 also target BAT with markers of impaired downstream lipolytic activation and increased accumulation of lipids; i.e., BAT becomes more beige/white. However, this inhibition is relative to the ambient conditions, since massive adrenergic activation by injecting the mice with a β3-agonist for 7 days activated BAT in both control and BMP4-treated mice, as evidenced by reduced lipids in both cohorts, albeit with still higher remaining lipid accumulation in BMP4 mice (Figure S1F). Lowering the room temperature to 4°C showed that the core body temperature

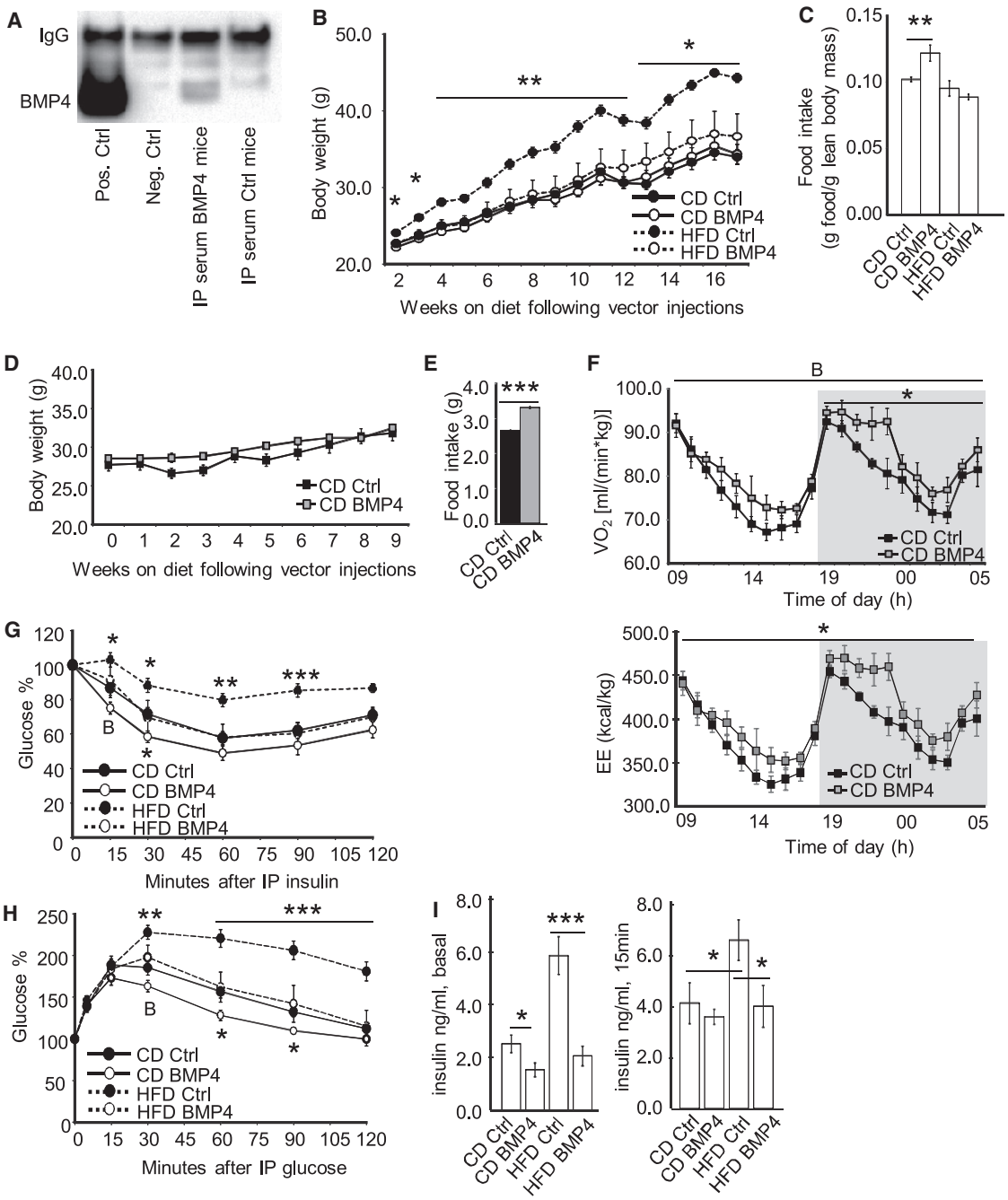

Figure 1. AAV BMP4 Treatment Reduces Weight Gain, Improves Glucose Tolerance, and Increases Energy Expenditure

(A) Immunoprecipitation of BMP4 from pooled serum (Figures S1A–S1C). IgG, immunoglobulin G.

(B) Weight gain in control-diet- and high-fat-diet-fed AAV BMP4 mice (CD/HFD BMP4; n = 11 each) and control groups (CD/HFD Ctrl; n = 20–21 each).

(C) Food intake normalized to lean body mass.

(D–F) Weight gain (D), absolute food intake (E), oxygen consumption (VO_2) and energy expenditure (both in F) in CD Ctrl and CD BMP4 mice from Cohort 2; n = 6 per group; see also Figures S1D and S1E.

(G and H) Insulin sensitivity (G) and glucose tolerance (H) in BMP4-treated mice and control groups. CD/HFD control (Ctrl), n = 20–21 each; CD/HFD BMP4, n = 11 each.

(I) Circulating insulin levels in BMP4-treated mice and control groups at baseline and 15 min post-glucose injection during the GTT; n = 5–9 (basal) and n = 8 (15 min).

In (A)–(C) and in (G)–(I), analyses were performed in mice from Cohort 1. In (B)–(I), data are indicated as mean ± SEM. *p < 0.05; **p < 0.01; ***p < 0.001. See also Figures S1A–S1E.

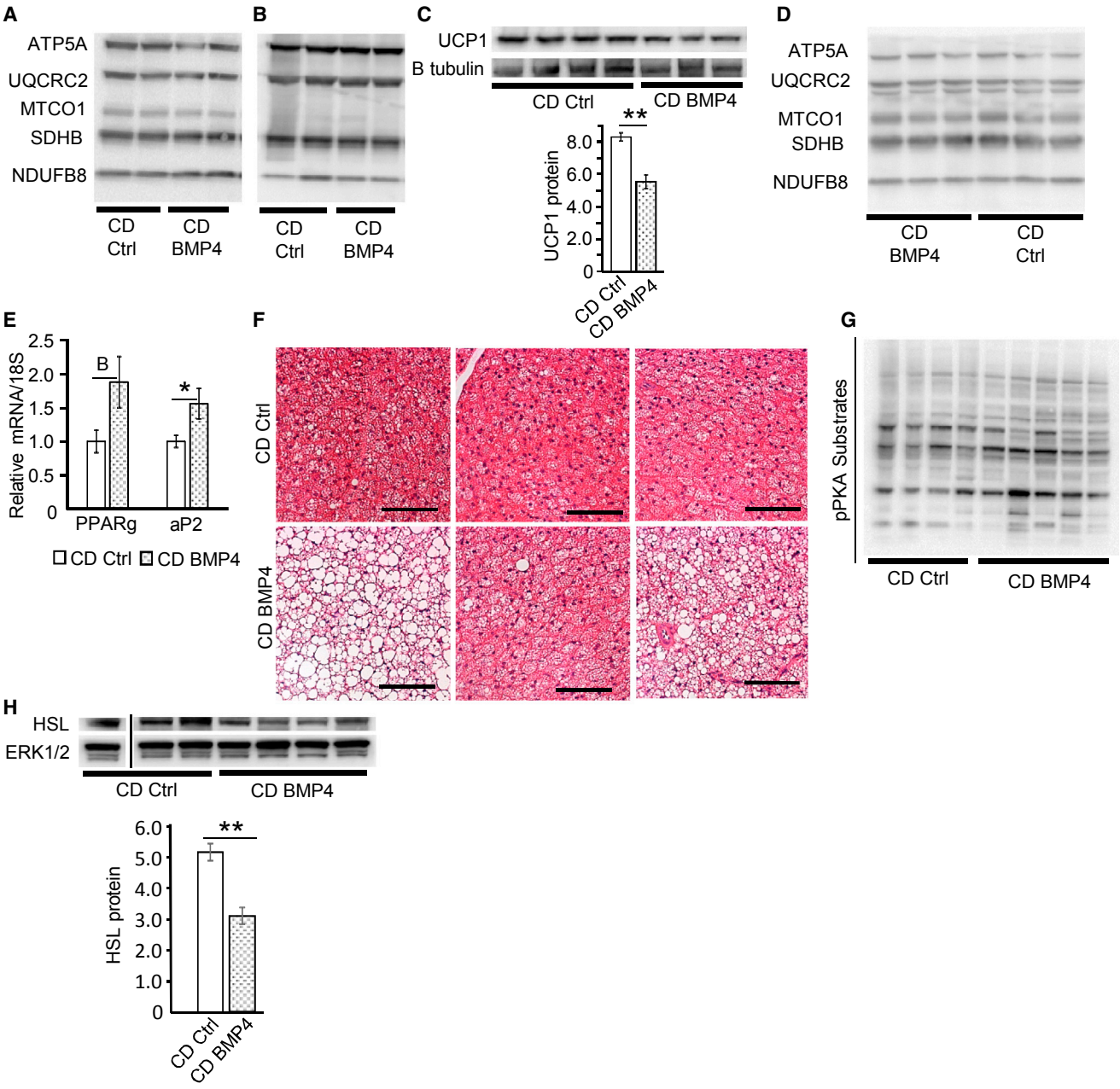

Figure 2. AAV BMP4 Treatment Enhances Lipid Accumulation and Reduces UCP1 Expression in BAT in CD-Fed Mice

(A and B) OXPHOS proteins in lysates from soleus (A) and gastrocnemius muscles (B) (both pooled).

(C and D) UCP1 protein (with quantification) (C) and OXPHOS proteins (D) in lysates from BAT.

(E) Gene expression of PPARγ and aP2 in BAT; n = 7–8 per group.

(F) Morphology of BAT in CD-fed BMP4 mice and controls (n = 3 per group). Scale bars, 100 μM.

(G and H) Phospho-protein kinase A (PKA) substrates (G) and HSL (with quantification) (H) in lysates from BAT.

All analyses were performed in mice from Cohort 1. The bar in (H) shows where a lane has been removed. In (C), (E), and (H), data are indicated as mean ± SEM. *$p < 0.05$; **$p < 0.01$.

See also Figure S1F.

was significantly higher in the BMP4-treated mice (Figure S1E), suggesting a functional activation of BAT in both groups but an additional contribution of the BMP4-induced browning of SubQ WAT as discussed later.

Elevated BMP4 Induces Browning of SubQ Adipose Tissue

Reduced oxidation, suggested by the BAT findings, is obviously not consistent with the increased whole-body energy

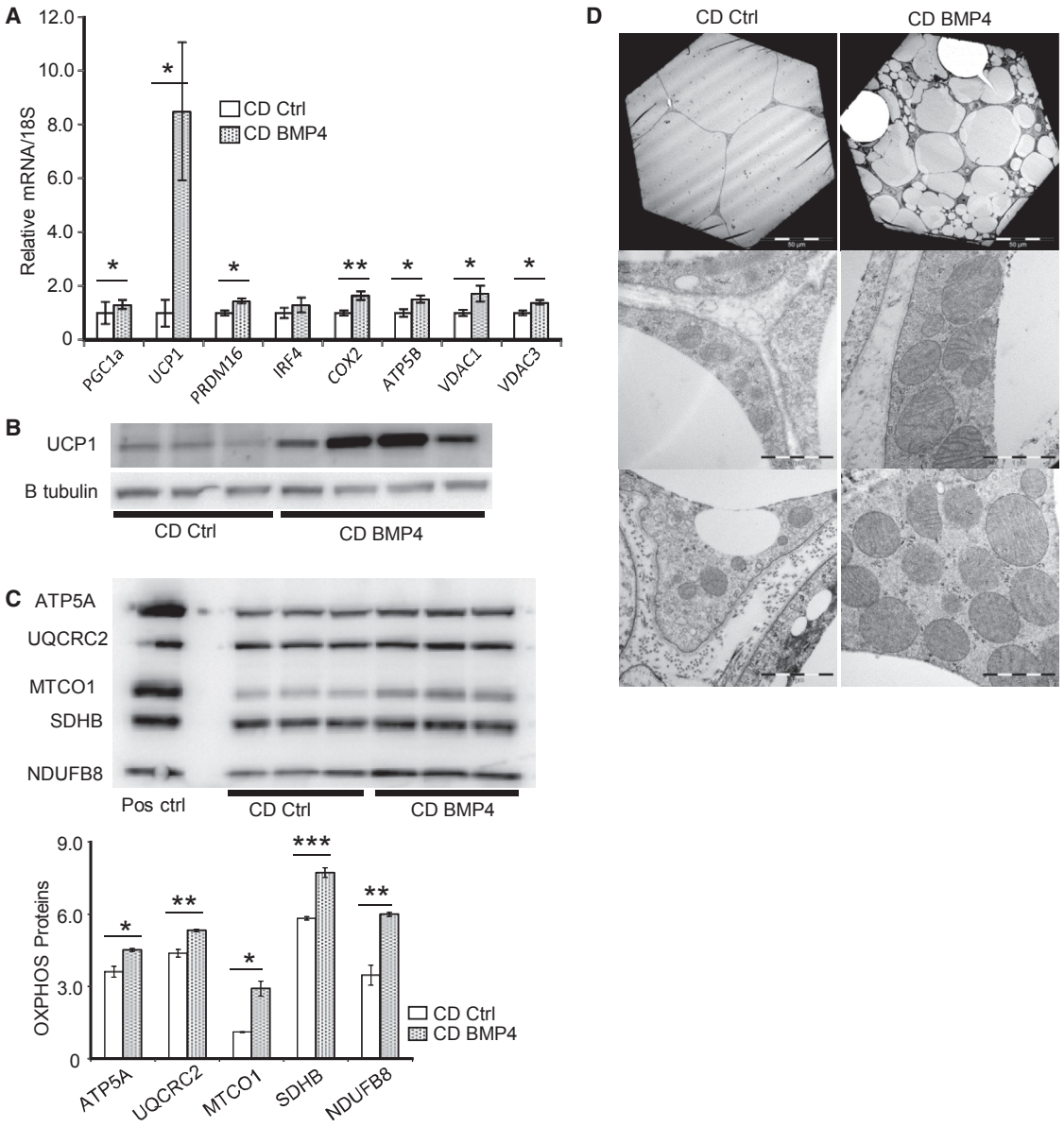

Figure 3. BMP4 Induces Browning of SubQ Fat in CD-Fed Mice

(A) Gene expression of beige fat and mitochondrial genes in SubQ fat from CD-fed BMP4 and control mice; n = 10–11 per group.

(B) UCP1 protein in pooled lysates from isolated SubQ adipocytes from BMP4 and control mice.

(C) OXPHOS proteins and quantification in pooled lysates from isolated SubQ adipocytes. n = 3 per group.

(D) Mitochondria in the SubQ fat in CD BMP4 mice and controls (Cohort 2), examined by electron microscopy. Representative images, total n = 3 per group. Scale bars, 50 μm (top) and 1 μm (center and bottom).

In (A)–(C), analyses were performed in mice from Cohort 1; data are indicated as mean ± SEM. *p < 0.05; **p < 0.01; ***p < 0.001.

expenditure in BMP4 animals. We then examined whether BMP4 targeted WAT to induce a beige/brown oxidative phenotype of the cells in these fully mature animals. Indeed, expression of a number of oxidative adipocyte genes (e.g., *Pgc1a*, *Ucp1*, PR Domain Containing 16 [Prdm16], and mitochondrial genes) were increased in the SubQ WAT of CD BMP4 mice (Figure 3A), which was also confirmed at the protein level with increased UCP1 protein in isolated and fully mature SubQ adipocytes (Figure 3B). Furthermore, OXPHOS proteins in isolated SubQ adipocytes from CD BMP4 mice were also significantly increased (Figure 3C). We also examined epididymal (EPI) fat and saw increased *Ucp1* expression as well, but this was markedly less pronounced than in SubQ fat (data not shown). To further document an increased oxidative capacity of the large SubQ fat, we examined mitochondria in the SubQ WAT using electron microscopy. As shown in Figure 3D, the mitochondria were larger, more densely expressed, and with increased cristae, supporting an effect of BMP4 on mitochondrial

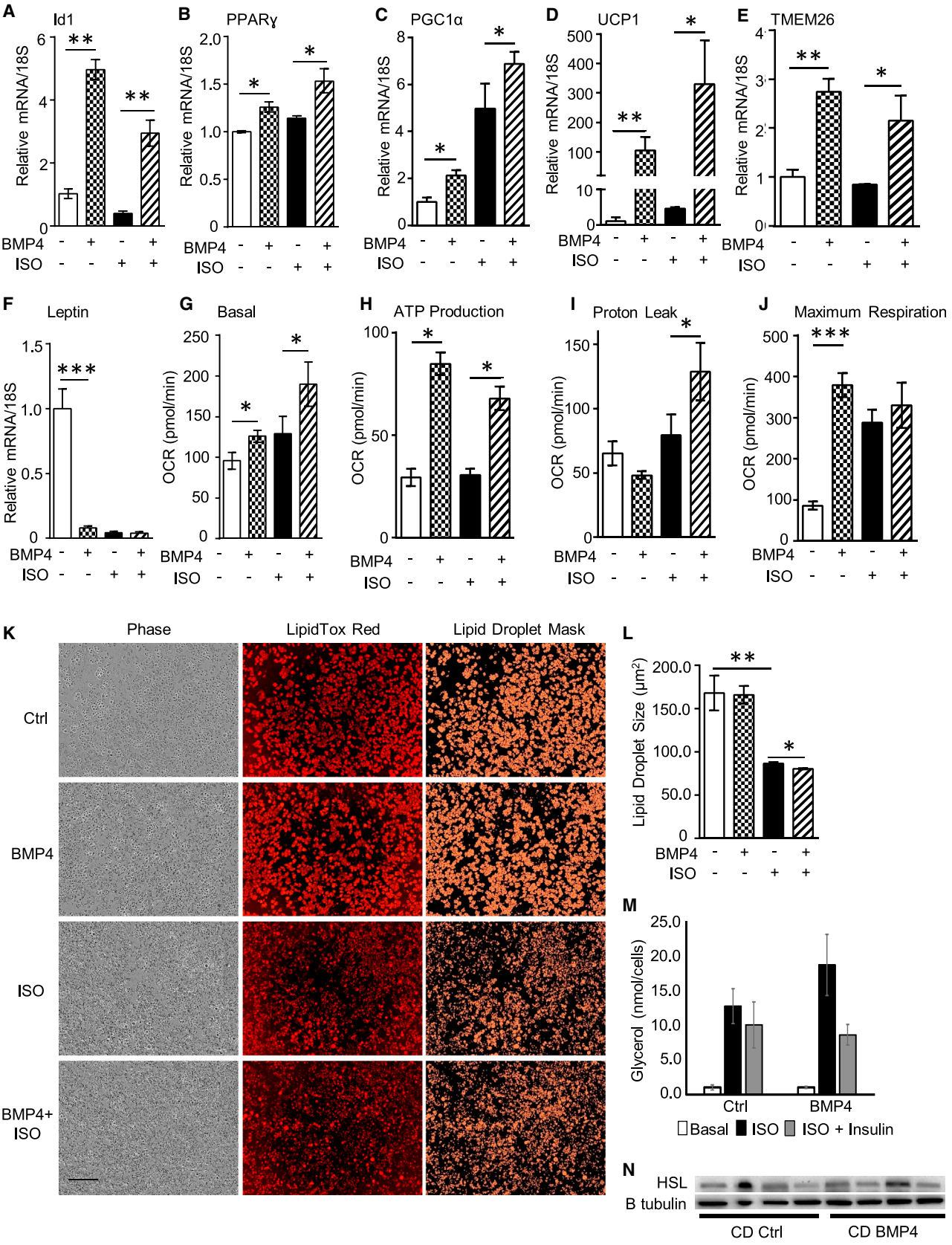

(legend on next page)

biogenesis and activation, consistent with the increased *Pgc1a* and OXPHOS proteins (Figures 3A and 3C). Together, our data show that SubQ WAT is a target of BMP4 in mature mice, which leads to increased browning, increased whole-body energy expenditure, and prevention of obesity, while BAT activation is reduced. Additionally, BMP4 treatment improves insulin sensitivity, even in the face of an unchanged body weight, which also is consistent with the increased thermogenic profile of WAT (Bartelt et al., 2011).

BMP4 Drives Browning of Differentiating Preadipocytes

In contrast to the procedures by Modica et al. (2016) in undifferentiated preadipocytes, we asked whether exogenous BMP4 treatment throughout adipocyte differentiation was associated with the induction of brown/beige adipocytes in vitro. The addition of exogenous BMP4 increased expression of the BMP-responsive genes *Id1* and *Pparg* (Figures 4A and 4B). Furthermore, beige/brown adipocyte markers *Pgc1α*, *Ucp1*, and Transmembrane protein 26 (*Tmem26*) were upregulated in response to exogenous BMP4 treatment, and this was further enhanced with the combination of BMP4 and adrenergic stimulation with isoproterenol (Figures 4C–4E). Interestingly, the white adipocyte marker leptin was downregulated in response to BMP4 and isoproterenol (Figure 4F).

To assess the functional consequence of exogenous BMP4, we measured cellular respiration in differentiated mouse preadipocytes both with and without 24-hr adrenergic stimulation with isoproterenol. We observed increased basal respiration, ATP production, and maximum respiration in response to BMP4, as compared to non-BMP4 treated adipocytes (Figures 4G–4J). Furthermore, adrenergic stimulation in combination with BMP4 increased basal respiration, ATP production, and uncoupled respiration, as compared to only isoproterenol-treated adipocytes (Figures 4G–4J).

Thus, we show that BMP4 drives the browning of WAT, both in vivo and in differentiating primary white precursor cells in vitro, resulting in functional, oxidative adipocytes. In contrast to findings of an impaired lipolysis and lipid oxidation in BAT cells, we show that the differentiating primary white precursor cells have unchanged lipid accumulation in the presence of BMP4 and that the isoproterenol-stimulated lipolysis is highly functional (Figures 4K and 4L). This was also seen in the isolated mature white SubQ adipocytes from CD-fed AAV BMP4 mice (Figure 4M). Additionally, HSL protein was not reduced in the SubQ WAT of BMP4-treated mice (Figure 4N). Together, these findings clearly document the different lipolytic responses to BMP4 in WAT and BAT.

SubQ WAT of HFD-Fed BMP4 Mice Also Shows Increased Browning

Body composition analysis showed that HFD BMP4 mice had reduced absolute body fat mass but unchanged lean body mass (Figure S2A). This was confirmed upon termination, showing significantly reduced weights of all studied WAT depots (Figure S2B) and significantly reduced adipocyte size (Figure S2C). Gene expression of inflammatory markers, including the macrophage marker *F4/80*, was reduced in HFD BMP4 mice, compared to HFD controls (Figure S2D), and this was confirmed by immunohistochemistry (Figure S2E).

Adipose tissue fibrosis is increased in hypertrophic obesity (Halberg et al., 2009; Khan et al., 2009), and BMPs have been reported to exert anti-fibrotic effects (Gao et al., 2014; Jenkins and Fraser, 2011; Zhong et al., 2013). Indeed, transcriptional activation of a number of known fibrotic genes was significantly reduced in the SubQ WAT of HFD BMP4 mice (Figure S2D), and Picosirius Red staining of collagen fibers was also reduced (data not shown). Ectopic fat accumulation in the livers of the HFD BMP4 mice, pronounced in the HFD control group, was virtually completely prevented by BMP4 (Figure S2F).

Similar to the findings in CD BMP4 mice, the SubQ adipose tissue of the HFD BMP4 mice had markedly increased numbers of UCP1-positive, multilobular adipocytes (Figure 5A), not seen in the HFD control mice. *Pgc1a*, *Tmem26*, and Interferon Regulatory Factor 4 (*Irf4*) mRNA levels were also increased (Figure 5B), as well as PGC1a protein levels (Figure 5C). *Pgc1a* mRNA in SubQ fat was significantly and negatively correlated with body weight in the HFD-fed mice (Figure 5D).

BMP4-Induced Browning of the SubQ WAT in Mature Mice—a Consequence of Transdifferentiation?

Browning of white adipocytes can occur through two principally separate events; either through differentiation of WAT-resident precursor cells (Qian et al., 2013; Wang et al., 2013) or by "transdifferentiation" of adipocytes and/or committed white precursor cells (Cinti, 2002; Himms-Hagen et al., 2000).

Adipose tissue cellularity is developed early; here, we injected mature mice with the AAV BMP4 vector (at 6 or 12 weeks of age) when the pool of precursor cells has since long been established (Wang et al., 2013). BMP4 has important developmental effects that may account for the increased browning of SubQ adipose tissue by the expansion of clones of beige precursor cells that underwent differentiation. We examined whether the number of adipose cells was increased (Figure 5E) but did not observe increased cellularity in either of the WAT depots in BMP4 mice, regardless of diet. Adipose precursor cells can have an endothelial origin (Tran et al., 2012); we, therefore, also measured

Figure 4. Differentiating Precursor Cells from SubQ Fat Undergo Browning with BMP4 Treatment

Primary SubQ preadipocytes differentiated for 7 days with BMP4 and isoproterenol (ISO) treatment.

(A–F) Gene expression; Id1 (A), PPARγ (B), PGC1α (C), UCP1 (D), TMEM26 (E), Leptin (F), n = 3 per group.

(G–J) Oxygen consumption rate (OCR) during basal respiration (G), ATP production (H), proton leak (I), and maximum respiration (J); n = 4 per group.

(K and L) Representative images of phase, lipid droplets (LipidTox Red), and analyzed lipid droplet mask (K) (scale bar, 300 μm) and quantification (L); n = 3 per group.

(M) Glycerol release of isolated SubQ adipocytes from control diet (CD)-fed control and BMP4 mice, with basal levels, following ISO and ISO + insulin treatment. n = 3 per group (pooled samples).

(N) HSL protein in lysates from SubQ fat from CD-fed mice.

Data are represented as mean ± SEM. *p < 0.05; **p < 0.01; ***p < 0.001.

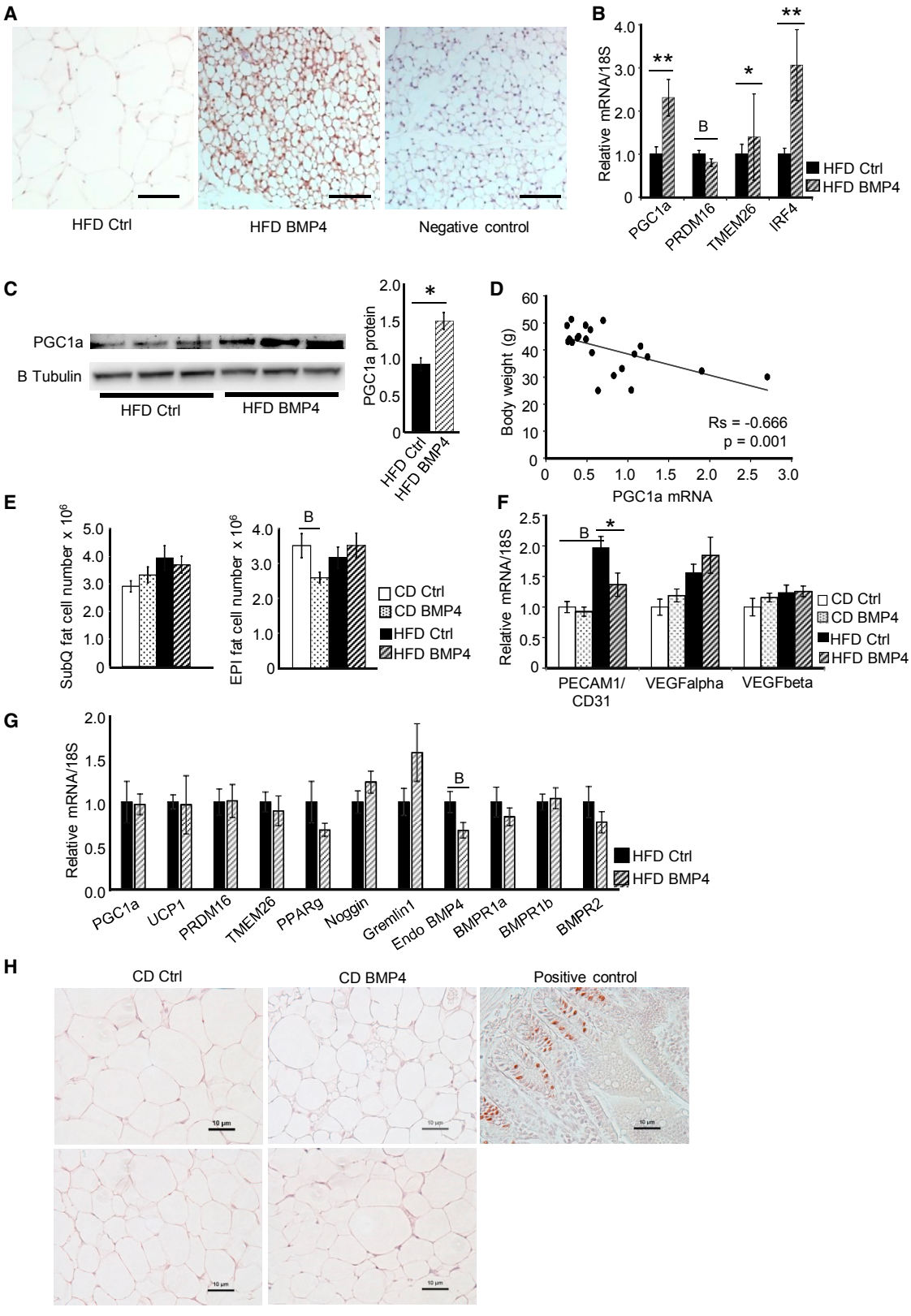

(legend on next page)

angiogenic and endothelial markers in the SubQ WAT. Again, there was no increase in the BMP4 mice on either diet (Figure 5F). We also isolated and characterized the undifferentiated adipocyte stromal vascular cells in the SubQ WAT but did not see markers of an increased beige phenotype in these precursor cells from animals treated with BMP4 (Figure 5G). We also measured bromodeoxyuridine (BrdU) incorporation in SubQ fat and found the same low incorporation in both groups (Figure 5H), further supporting transdifferentiation rather than specific clonal expansion of beige/brown cells, Taken together, the data show that BMP4 can target cells undergoing differentiation and "transdifferentiate" them into an oxidative beige phenotype and that this may also be possible with mature cells in vivo. However, definitive in vivo proof requires studies where the precursor cells have been genetically labeled.

Hypertrophic Obesity in Mice Is Characterized by Cellular BMP4 Resistance and Increased Noggin

Several markers of an oxidative beige phenotype in the SubQ adipose tissue, including *Irf4* and *Tmem26*, were reduced in non-BMP4-treated, HFD mice, compared to CD mice, as was also reported previously in obesity (Kong et al., 2014). Considering our present findings of the effects of BMP4 in inducing an oxidative beige phenotype of the SubQ adipose tissue, we examined whether BMP4 and/or its downstream signaling are reduced in HFD-fed mice.

Similar to our previous findings in human cells (Gustafson et al., 2015), obese HFD-fed control mice had increased endogenous *Bmp4* in SubQ WAT (Figure S3A), compared to lean mice. *Bmp4* mRNA levels also correlated positively with adipocyte size (Figure S3B) and tended to correlate with body weight and circulating insulin levels. Since this is inconsistent with the reduced markers of SubQ browning in HFD, we examined the expression pattern of endogenous BMP4 antagonists in lean and obese mice. The increased BMP4 in HFD mice was accompanied by both increased gene and protein expression of the BMP antagonist Noggin (Figures S3A and S3E), but not, like in human adipose tissue, Gremlin1 (Gustafson et al., 2015). Noggin mRNA levels in the SubQ WAT correlated positively with SubQ adipocyte size, body weight, and circulating insulin levels (Figure S3C). This association was not found for Gremlin1 (Figure S3D). The concept of a cellular BMP4 resistance in SubQ adipose tissue in obesity was further supported by the reduced endogenous pSMAD1/5/8 in adipose cells from HFD mice, compared to CD mice, but its restoration in HFD BMP4 mice (Figure S3F).

DISCUSSION

The present study was designed as a follow-up of our recent findings that differentiating human SubQ adipose precursor cells assume a beige/brown and oxidative phenotype when cultured in the presence of BMP4 and/or following silencing Gremlin1, the predominant endogenous BMP antagonist in these cells (Gustafson et al., 2015).

Here, we focused on the potential effect of increased BMP4 signaling/action in treating/preventing obesity in fully mature mice. For this to become an interesting potential therapeutic option, it is critical to investigate the effect in mature models, since such therapy would only be initiated in human adults. This approach may also account for the differences seen in our model compared to findings in transgenic mice overexpressing *Bmp4* in the adipose tissue. These mice had increased BAT mass, also seen in transgenic mice overexpressing *Bmp7* (Tseng et al., 2008), but this was mainly due to increased lipid droplets (Qian et al., 2013), and similar results were recently reported in an extensive characterization of the effects of BMP4 on brown adipose cell differentiation in vitro (Modica et al., 2016). The mechanisms for this were attributed to reduced lipolytic activation of HSL in the brown adipose cells. This was further validated by injecting adenoviruses that increased BMP4 in BAT in the mice. However, in marked contrast to these data, but not further addressed or discussed, Modica et al. (2016) also reported that systemically injected BMP4 *increased energy expenditure* in the mice, and this is obviously in complete contrast to their findings in BAT and brown cell development. Our results clearly show that SubQ WAT is a positive target of BMP4, leading to increased browning and increased whole-body energy expenditure, which was seen regardless of the increased lipid accumulation in BAT and its reduced ability to oxidize lipids.

We favor the interpretation of the data reported in BAT (Modica et al., 2016), together with our present and previous results (Gustafson et al., 2015), that BMP4 enhances the development of a beige/brown phenotype in both brown and white adipose cells, a likely consequence of the enhanced *PPARg* activation and associated downstream genes (Gustafson et al., 2015).

The increased lipid accumulation and beige phenotype of BAT in BMP4-treated mice was seen under normal room temperature and without any direct exogenous activation of the adrenergic system. However, when we treated the mice with either a β3 agonist for 7 days or with lowering the temperature, BAT became clearly activated, as evidenced by the marked reduction in lipids and higher core temperature. The higher

Figure 5. BMP4 Induces Browning of the SubQ Fat without Evidence of Recruiting New Precursor Cells

(A) UCP1 immunostaining in SubQ fat; n = 5 per group. Scale bars, 100 μm.

(B–D) Gene expression of beige/brown genes in SubQ fat (n = 10–11 per group) (B) and PGC1a protein in pooled SubQ fat lysates (C). In (D), *Pgc1a* mRNA in SubQ fat is negatively correlated with body weight in high-fat diet (HFD)-fed mice; n = 21.

(E) Adipocyte number in SubQ (left) and epididymal (EPI, right) fat in BMP4 mice, compared to Ctrl groups. Control diet (CD)/HFD Ctrl, n = 20–21 each; CD/HFD BMP4, n = 11 each.

(F and G) Gene expression of endothelial marker genes in SubQ fat (n = 9–11 per group) (F) and of beige fat- and BMP-related genes in undifferentiated stromal vascular cells (n = 6–10 per group) (G).

(H) BrDU staining of proliferating cells in sections of SubQ fat from CD-fed BMP4 and control mice (Cohort 2), and positive control (gut). Scale bars, 10 μm.

In (A)–(G), analyses were performed in mice from Cohort 1, but the mice used in (G) were terminated at week 12, after vector injections. In (B), (C), and (E–G), data are indicated as mean ± SEM. B = $p < 0.1$; *$p < 0.05$; **$p < 0.01$; and ***$p < 0.001$.

See also Figures S2 and S3.

core temperature is likely a reflection of activating both BAT and the oxidative beige/brown SubQ WAT. The BMP4-mediated effect on inhibiting lipolysis in BAT is interesting, as the white adipose cells exhibit no decrease in ability to mobilize lipids in response to β-adrenergic stimulation.

There was no difference in weight gain in the CD BMP4 compared to control mice, in spite of their increased energy expenditure, but they also had increased food intake. It is currently unknown whether BMP4 has any direct effect on food intake in mice, but intra-cerebroventricular injection of BMP7 leads to decreased food intake in several different obese mouse models (Townsend et al., 2012). However, BMP2, which is essentially similar in most respects to BMP4, did not have any direct effects on food intake (Townsend et al., 2012).

Interestingly, CD BMP4 mice showed evidence of increased insulin sensitivity and an improved glucose tolerance, although their body weights were almost identical to those of the control mice. It has previously been shown that thermogenic activation of the adipose cells leads to increased insulin sensitivity and an improved metabolic profile (Bartelt and Heeren, 2014; Bartelt et al., 2017), but whether this is due to endocrine effects of secreted molecules by the beige adipose tissue and/or direct effects of BMP4 on insulin signaling/action is currently unclear and under investigation. However, we examined both the expression of markers of the futile creatine pathway and the thermogenic *Slit2* fragment but saw no change in either of these (data not shown).

Regarding the mode of action for BMP4-induced browning of SubQ WAT, a recent extensive study demonstrated that ZFP423 acts as a molecular brake on adipocyte thermogenesis by inhibiting the brown-fat transcription factor EBF2 in white adipocytes (Shao et al., 2016). Mechanistically, BMP4 and BMP7 were shown to dissociate the ZFP423-EBF2 complex, allowing EBF2 to drive the thermogenic gene program (Shao et al., 2016). This is a potential and attractive mechanism and indicates peripheral pathways for browning WAT rather than direct adrenergic activation in the present AAV BMP4 mouse model.

Interestingly, HSL protein was not reduced, and induction of isoproterenol-stimulated lipolysis in WAT tended to be higher in the BMP4-treated mice (Figures 4M and 4N). Thus, we cannot exclude that BMP4 enhances downstream sensitivity/response to cellular adrenergic activation in WAT. A recent study identified that deletion of the cyclic AMP (cAMP)-degrading enzyme PDE3B in the adipose tissue also enhanced browning of the SubQ fat, increased energy expenditure, and protected the mice from HFD-induced obesity (Chung et al., 2017). However, further studies are needed to examine central and peripheral effects of BMP4, which can account for the increased thermogenesis in the SubQ WAT in vivo.

The inverse regulation of BAT and SubQ WAT by BMP4 is intriguing and can be a direct consequence of the increased BMP4 secretion by the large SubQ WAT, targeting BAT and reducing its ability to mobilize and oxidize lipids. It may well also be the explanation why human BAT is mainly of the beige-/white-like phenotype and why obese individuals have been reported to have lower activation of BAT (Wu et al., 2012; Cypess et al., 2009). This would, then, not be a direct causal effect of an impaired BAT activation in obesity but, rather, secondary to the increased WAT and its secretion of BMP4.

In addition, we conclude here that the use of BMP4 itself in obesity may present a problem since our data, like in human adipose cells (Gustafson et al., 2015), also document the presence of cellular resistance to BMP4 in the adipose tissue in obesity that needs to be overcome. Together, these findings suggest that antagonizing the secreted endogenous BMP inhibitors may be a preferable approach.

EXPERIMENTAL PROCEDURES

Animals

C57BL6/N male mice (Taconic, Hudson, NY, USA) were group caged, maintained on a 12-hr/12-hr light/dark cycle in a temperature (+21°C)- and humidity-controlled room. Food and drinking water were administered ad libitum, and the mice were fed a high-fat diet (HFD; 45 kcal% fat) or a nutrient-matched control diet (CD; 10 kcal% fat, both from Research Diets, New Brunswick, NJ, USA). Food intake was recorded daily over 1 week. Two separate cohorts of mice were included (Figures S4A and S4B). In Cohort 1, initially lean 6-week-old mice were injected with AAV BMP4 vectors and fed a CD or an HFD for 17 weeks. In Cohort 2, the vectors were injected in 12-week-old mice and fed a CD for 9 weeks. A subgroup of the HFD-fed mice received daily intraperitoneal injections with the β3-adrenergic agonist CL-316 243 (1 mg/kg; Sigma Aldrich, St. Louis, MO, USA) or vehicle for 7 days prior to termination. All animal experiments were approved by the Research Animal Ethics Committee at the University of Gothenburg, Sweden.

Recombinant AAV Vectors and In Vivo Administration

Recombinant AAV vectors of serotype 8 encoding a codon-optimized murine *Bmp4* cDNA sequence under control of the human Alpha 1-Antitrypsin (*hAAT1)* promoter were produced in HEK293 cells and then purified as described earlier (Ayuso et al., 2010). A non-coding plasmid carrying the *hAAT1* promoter was used to produce empty vectors for control mice. The mice received AAV vectors (5×10^{11} viral particles per 200 μL saline per mouse), either via retro-orbital (cohort1) or lateral tail venous injection (cohort2). The study diets were started concurrently with the AAV injections ("week 0" in Figures S4A and S4B).

Figures and Statistical Calculations

Results are reported as means ± SEM. Significances are indicated in the figures according to the following: B = $p < 0.1$, *$p < 0.05$, **$p < 0.01$, and ***$p < 0.001$. Statistics were performed using IBM SPSS Statistics v20 or GraphPad Prism v6.03 for Windows. Pairwise comparisons were performed using the Mann-Whitney non-parametric U test, Student's t test, or one-way ANOVA as appropriate. Spearman's nonparametric correlation coefficient was used to measure dependence between variables.

Further description of the experimental procedures is given in the Supplemental Information.

SUPPLEMENTAL INFORMATION

Supplemental Information includes Supplemental Experimental Procedures and four figures and can be found with this article online at http://dx.doi.org/10.1016/j.celrep.2017.07.020.

AUTHOR CONTRIBUTIONS

U.S., S.H., J.M.H., C.C., and A.H. designed the experiments; J.M.H. and J.R.G. performed animal husbandry and mouse in vivo experiments, and J.M.H., S.H., C.C., and A.H. did the cell work. F.B. and I.E. generated and characterized the viral vectors, and J.-O.J. and V.P. contributed to the energy expenditure and activity measurements. U.S. and J.M.H. wrote the final article, and all authors approved and contributed.

ACKNOWLEDGMENTS

We thank our colleagues at the Lundberg Laboratory for Diabetes Research for fruitful discussions. We are grateful for technical assistance from the Laboratory for Experimental Biomedicine, where all animal experiments took place.

This work was funded by the Swedish Research Council, the Swedish Diabetes Association, the Novo Nordisk Foundation, the Torsten Söderberg Foundation, the Wilhelm and Martina Lundgren Foundation, the Edgar Sjölund Foundation, the Inga Britt and Arne Lundberg Foundation, the West Sweden ALF program, and an EFSD/Lilly research grant. F.B. is an ICREA Academia recipient, Generalitat de Catalunya, Spain, and funded by the Ministerio de Economía y Competitividad (SAF 2014-54866-R), Spain.

Received: January 13, 2017
Revised: May 10, 2017
Accepted: July 10, 2017
Published: August 1, 2017

REFERENCES

Anguela, X.M., Tafuro, S., Roca, C., Callejas, D., Agudo, J., Obach, M., Ribera, A., Ruzo, A., Mann, C.J., Casellas, A., and Bosch, F. (2013). Nonviral-mediated hepatic expression of IGF-I increases Treg levels and suppresses autoimmune diabetes in mice. Diabetes *62*, 551–560.

Ayuso, E., Mingozzi, F., Montane, J., Leon, X., Anguela, X.M., Haurigot, V., Edmonson, S.A., Africa, L., Zhou, S., High, K.A., et al. (2010). High AAV vector purity results in serotype- and tissue-independent enhancement of transduction efficiency. Gene Ther. *17*, 503–510.

Bartelt, A., and Heeren, J. (2014). Adipose tissue browning and metabolic health. Nat. Rev. Endocrinol. *10*, 24–36.

Bartelt, A., Bruns, O.T., Reimer, R., Hohenberg, H., Ittrich, H., Peldschus, K., Kaul, M.G., Tromsdorf, U.I., Weller, H., Waurisch, C., et al. (2011). Brown adipose tissue activity controls triglyceride clearance. Nat. Med. *17*, 200–205.

Bartelt, A., John, C., Schaltenberg, N., Berbée, J.F.P., Worthmann, A., Cherradi, M.L., Schlein, C., Piepenburg, J., Boon, M.R., Rinninger, F., et al. (2017). Thermogenic adipocytes promote HDL turnover and reverse cholesterol transport. Nat. Commun. *8*, 15010.

Bowers, R.R., and Lane, M.D. (2007). A role for bone morphogenetic protein-4 in adipocyte development. Cell Cycle *6*, 385–389.

Chung, Y.W., Ahmad, F., Tang, Y., Hockman, S.C., Kee, H.J., Berger, K., Guirguis, E., Choi, Y.H., Schimel, D.M., Aponte, A.M., et al. (2017). White to beige conversion in PDE3B KO adipose tissue through activation of AMPK signaling and mitochondrial function. Sci. Rep. *7*, 40445.

Cinti, S. (2002). Adipocyte differentiation and transdifferentiation: plasticity of the adipose organ. J. Endocrinol. Invest. *25*, 823–835.

Cypess, A.M., Lehman, S., Williams, G., Tal, I., Rodman, D., Goldfine, A.B., Kuo, F.C., Palmer, E.L., Tseng, Y.H., Doria, A., et al. (2009). Identification and importance of brown adipose tissue in adult humans. N. Engl. J. Med. *360*, 1509–1517.

Gao, X., Cao, Y., Staloch, D.A., Gonzales, M.A., Aronson, J.F., Chao, C., Hellmich, M.R., and Ko, T.C. (2014). Bone morphogenetic protein signaling protects against cerulein-induced pancreatic fibrosis. PLoS ONE *9*, e89114.

Gustafson, B., and Smith, U. (2012). The WNT inhibitor Dickkopf 1 and bone morphogenetic protein 4 rescue adipogenesis in hypertrophic obesity in humans. Diabetes *61*, 1217–1224.

Gustafson, B., Hammarstedt, A., Hedjazifar, S., Hoffmann, J.M., Svensson, P.A., Grimsby, J., Rondinone, C., and Smith, U. (2015). BMP4 and BMP antagonists regulate human white and beige adipogenesis. Diabetes *64*, 1670–1681.

Halberg, N., Khan, T., Trujillo, M.E., Wernstedt-Asterholm, I., Attie, A.D., Sherwani, S., Wang, Z.V., Landskroner-Eiger, S., Dineen, S., Magalang, U.J., et al. (2009). Hypoxia-inducible factor 1alpha induces fibrosis and insulin resistance in white adipose tissue. Mol. Cell. Biol. *29*, 4467–4483.

Himms-Hagen, J., Melnyk, A., Zingaretti, M.C., Ceresi, E., Barbatelli, G., and Cinti, S. (2000). Multilocular fat cells in WAT of CL-316243-treated rats derive directly from white adipocytes. Am. J. Physiol. Cell Physiol. *279*, C670–C681.

Jenkins, R.H., and Fraser, D.J. (2011). BMP-6 emerges as a potential major regulator of fibrosis in the kidney. Am. J. Pathol. *178*, 964–965.

Jespersen, N.Z., Larsen, T.J., Peijs, L., Daugaard, S., Homøe, P., Loft, A., de Jong, J., Mathur, N., Cannon, B., Nedergaard, J., et al. (2013). A classical brown adipose tissue mRNA signature partly overlaps with brite in the supraclavicular region of adult humans. Cell Metab. *17*, 798–805.

Kazak, L., Chouchani, E.T., Jedrychowski, M.P., Erickson, B.K., Shinoda, K., Cohen, P., Vetrivelan, R., Lu, G.Z., Laznik-Bogoslavski, D., Hasenfuss, S.C., et al. (2015). A creatine-driven substrate cycle enhances energy expenditure and thermogenesis in beige fat. Cell *163*, 643–655.

Khan, T., Muise, E.S., Iyengar, P., Wang, Z.V., Chandalia, M., Abate, N., Zhang, B.B., Bonaldo, P., Chua, S., and Scherer, P.E. (2009). Metabolic dysregulation and adipose tissue fibrosis: role of collagen VI. Mol. Cell. Biol. *29*, 1575–1591.

Kong, X., Banks, A., Liu, T., Kazak, L., Rao, R.R., Cohen, P., Wang, X., Yu, S., Lo, J.C., Tseng, Y.H., et al. (2014). IRF4 is a key thermogenic transcriptional partner of PGC-1α. Cell *158*, 69–83.

Modica, S., Straub, L.G., Balaz, M., Sun, W., Varga, L., Stefanicka, P., Profant, M., Simon, E., Neubauer, H., Ukropcova, B., et al. (2016). Bmp4 promotes a brown to white-like adipocyte shift. Cell Rep. *16*, 2243–2258.

Qian, S.W., Tang, Y., Li, X., Liu, Y., Zhang, Y.Y., Huang, H.Y., Xue, R.D., Yu, H.Y., Guo, L., Gao, H.D., et al. (2013). BMP4-mediated brown fat-like changes in white adipose tissue alter glucose and energy homeostasis. Proc. Natl. Acad. Sci. USA *110*, E798–E807.

Seale, P., Bjork, B., Yang, W., Kajimura, S., Chin, S., Kuang, S., Scimè, A., Devarakonda, S., Conroe, H.M., Erdjument-Bromage, H., et al. (2008). PRDM16 controls a brown fat/skeletal muscle switch. Nature *454*, 961–967.

Seale, P., Conroe, H.M., Estall, J., Kajimura, S., Frontini, A., Ishibashi, J., Cohen, P., Cinti, S., and Spiegelman, B.M. (2011). Prdm16 determines the thermogenic program of subcutaneous white adipose tissue in mice. J. Clin. Invest. *121*, 96–105.

Shao, M., Ishibashi, J., Kusminski, C.M., Wang, Q.A., Hepler, C., Vishvanath, L., MacPherson, K.A., Spurgin, S.B., Sun, K., Holland, W.L., et al. (2016). Zfp423 maintains white adipocyte identity through suppression of the beige cell thermogenic gene program. Cell Metab. *23*, 1167–1184.

Sidossis, L.S., Porter, C., Saraf, M.K., Børsheim, E., Radhakrishnan, R.S., Chao, T., Ali, A., Chondronikola, M., Mlcak, R., Finnerty, C.C., et al. (2015). Browning of subcutaneous white adipose tissue in humans after severe adrenergic stress. Cell Metab. *22*, 219–227.

Svensson, K.J., Long, J.Z., Jedrychowski, M.P., Cohen, P., Lo, J.C., Serag, S., Kir, S., Shinoda, K., Tartaglia, J.A., Rao, R.R., et al. (2016). A secreted Slit2 fragment regulates adipose tissue thermogenesis and metabolic function. Cell Metab. *23*, 454–466.

Townsend, K.L., Suzuki, R., Huang, T.L., Jing, E., Schulz, T.J., Lee, K., Taniguchi, C.M., Espinoza, D.O., McDougall, L.E., Zhang, H., et al. (2012). Bone morphogenetic protein 7 (BMP7) reverses obesity and regulates appetite through a central mTOR pathway. FASEB J. *26*, 2187–2196.

Tran, K.V., Gealekman, O., Frontini, A., Zingaretti, M.C., Morroni, M., Giordano, A., Smorlesi, A., Perugini, J., De Matteis, R., Sbarbati, A., et al. (2012). The vascular endothelium of the adipose tissue gives rise to both white and brown fat cells. Cell Metab. *15*, 222–229.

Tseng, Y.H., Kokkotou, E., Schulz, T.J., Huang, T.L., Winnay, J.N., Taniguchi, C.M., Tran, T.T., Suzuki, R., Espinoza, D.O., Yamamoto, Y., et al. (2008). New role of bone morphogenetic protein 7 in brown adipogenesis and energy expenditure. Nature *454*, 1000–1004.

Vitali, A., Murano, I., Zingaretti, M.C., Frontini, A., Ricquier, D., and Cinti, S. (2012). The adipose organ of obesity-prone C57BL/6J mice is composed of mixed white and brown adipocytes. J. Lipid Res. *53*, 619–629.

Wang, Q.A., Tao, C., Gupta, R.K., and Scherer, P.E. (2013). Tracking adipogenesis during white adipose tissue development, expansion and regeneration. Nat. Med. *19*, 1338–1344.

Wu, J., Boström, P., Sparks, L.M., Ye, L., Choi, J.H., Giang, A.H., Khandekar, M., Virtanen, K.A., Nuutila, P., Schaart, G., et al. (2012). Beige adipocytes are a distinct type of thermogenic fat cell in mouse and human. Cell *150*, 366–376.

Zhong, L., Wang, X., Wang, S., Yang, L., Gao, H., and Yang, C. (2013). The anti-fibrotic effect of bone morphogenic protein-7(BMP-7) on liver fibrosis. Int. J. Med. Sci. *10*, 441–450.

Zincarelli, C., Soltys, S., Rengo, G., and Rabinowitz, J.E. (2008). Analysis of AAV serotypes 1-9 mediated gene expression and tropism in mice after systemic injection. Mol. Ther. *16*, 1073–1080.